

New experimental equipment for grazing-exit electron-probe microanalysis

著者	Tsuji K., Spolnik Z., Ashino T.
journal or publication title	Review of Scientific Instruments
volume	72
number	10
page range	3933-3936
year	2001
URL	http://hdl.handle.net/10097/53413

doi: 10.1063/1.1405788

New experimental equipment for grazing-exit electron-probe microanalysis

K. Tsuji,^{a)} Z. Spolnik, and T. Ashino

Institute for Materials Research, Tohoku University, 2-1-1 Katahira, Aoba, Sendai 980-8577, Japan

(Received 30 January 2001; accepted for publication 16 July 2001)

New grazing-exit electron-probe microanalysis (GE-EPMA) equipment is developed. In GE-EPMA, characteristic x rays are measured at the grazing-exit angle. X rays emitted from deep positions in the substrate are reduced under grazing-exit conditions; therefore, surface-sensitive analysis is possible with low background. In previous equipments, the sample holder was tilted to change the exit angle. In this new equipment, the energy-dispersive x-ray detector is moved to change the exit angle, and the analyzed position is stable even if the exit angle is changed. Therefore, this equipment is useful especially for particle analysis. The new GE-EPMA equipment is applied to Pd–Se–Te single-particle analysis. Although it was difficult to measure the Se $K\alpha$ line at an exit angle of 45° due to the large Au $L\beta$ radiation emitted from the Au substrate, Se $K\alpha$ was measured without any Au signals at the grazing-exit angle near zero. © 2001 American Institute of Physics.

[DOI: 10.1063/1.1405788]

I. INTRODUCTION

Electron-probe microanalysis (EPMA) is a well-known method for localized analysis.¹ It is easy to use an electron probe of small diameter of less than $1\ \mu\text{m}$, although the minimum diameter of an x-ray microprobe used in x-ray fluorescence analysis is about $10\ \mu\text{m}$. There are many applications of EPMA to quantitative analysis.^{2–5} Electron-induced characteristic x rays are emitted in the region from the surface to the depth of about $1–2\ \mu\text{m}$, depending on the type of materials and the accelerating voltage of the electron beam. Since the analyzed depth of a few μm is too large, EPMA is not considered as a surface analytical method. There are some requests of surface analysis using EPMA, a secondary electron microscope (SEM) energy-dispersive x-ray spectrometer (EDS) in the field of the semiconductor industry. So far, surface analysis of EPMA has been performed by using low-energy electrons,^{6–8} because the penetration depth of the electron beam becomes small as the electron energy decreases. However, in this case, analytical x-ray lines in the energy region more than the accelerating voltage cannot be used. It is also important to investigate small particles on Si wafers in the manufacturing process of semiconductor devices, because such particles affect the properties of the devices. When the diameter of the particles is very small, electrons easily pass through the particle, and then strong characteristic and continuous background x rays are emitted from the Si wafer. These x rays disturb particle analysis.

The recently developed grazing-exit EPMA (GE EPMA) would be an answer for the above-mentioned requests.^{9–11} In GE EPMA, characteristic x rays are measured at small take-off (grazing-exit) angles. X rays emitted from deep positions in the sample are strongly absorbed in the long path to the detector. In addition, these x rays are refracted at the surface¹² and they are cut by the sides of the slits placed in

front of the x-ray detector. Therefore, only the x rays emitted from the surface are measured under grazing-exit conditions. It is also possible to measure a small single particle on a substrate with low background.¹³

II. EXPERIMENTAL ARRANGEMENTS FOR GE EPMA

It is a key point to control the exit angle in GE-EPMA measurements. To change the exit angle, we can consider two experimental setups, as shown in Fig. 1. In the first experimental arrangement [Fig. 1(a)], the sample holder is tilted to change the exit angle, and the EDS is fixed (stable). The commercially available EPMA (or SEM-EDS) has a function to tilt the sample holder, and the x-ray detector is usually strictly connected to the vacuum chamber. Therefore, it is easy to apply the first setup [Fig. 1(a)] to the conventional EPMA apparatus. However, if the sample surface is not placed exactly on the center of rotation, the analyzed position moves when the sample stage is tilted. The incident angle is also changed by tilting the sample holder. Actually, it is very difficult to set the analyzed position exactly at the center of rotation. Therefore, this arrangement is not suitable for localized analysis and single-particle analysis.

In the second setup shown in Fig. 1(b), the EDS is moved to change the exit angle instead of tilting the sample. Therefore, the analyzed position is stable. This is a merit, especially for particle analysis. However, the x-ray detector has to be fixed on a z-axis translation stage, and it has to be connected to the vacuum chamber of the SEM using a flexible tube. In this article, recently developed GE-EPMA equipment of the second type is introduced, and its application to single-particle analysis of Pd–Se–Te is shown.

III. EXPERIMENTAL SETUP

Figure 2 shows the experimental setup of the new GE-EPMA equipment, which consists of the SEM (JSM-5500, JEOL, Japan) and the EDS (high-purity Si detector, Horiba, Japan). The electron beam (accelerating voltage: 20 kV) ir-

^{a)}Electronic mail: tsuji@imr.tohoku.ac.jp

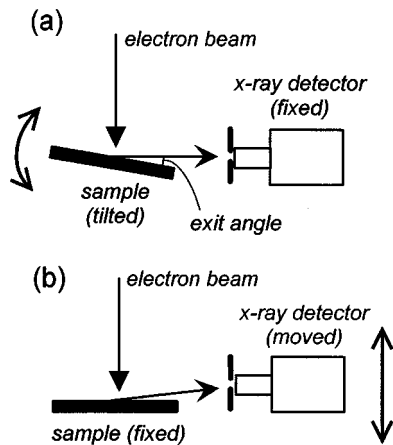


FIG. 1. Experimental arrangements of GE EPMA. Characteristic x rays exited by electron beam are detected at grazing-exit angles. (a) To change the exit angle, the sample holder is tilted. (b) The x-ray detector is moved.

radiated the sample at a right angle. The characteristic x rays were measured at a direction of 90° from the electron beam. The distance between the sample and the top of the EDS was 85 mm. A slit (0.5 mm in width) was attached on the top of the EDS. This slit consists of two Ta plates, and the width of this slit is adjustable. The divergence for x-ray detection depends on both the slit width and the distance between the sample and the EDS. In the case where the slit width is 0.5 mm and the distance is 85 mm, the divergence is about 0.34° . This is enough to distinguish between the x rays emitted from the surface and the x rays emitted from the substrate.

The EDS was attached to the vacuum chamber of the SEM using a flexible stainless-steel tube. The flexible tube makes it possible to move the EDS in the vacuum. Since the flexible tube is shrunk in the vacuum, the tube loses its flexibility. Thus, as shown in Fig. 3, two stainless-steel bars (props) were attached parallel to the flexible tube. Two linear movement guides were also attached to the ends of the two bars. Therefore, the EDS can be moved up and down keeping the distance between the SEM and the EDS constant.

The EDS was placed on a z-axis stage (ZA10-03, Kohzu, Japan), which was controlled with a stepping motor (minimum step: $0.5 \mu\text{m}$). A computer controlled both the stepping motor and the multichannel analyzer (MCA98-B, Laboratory Equipment, Japan). The exit-angle dependence of the char-

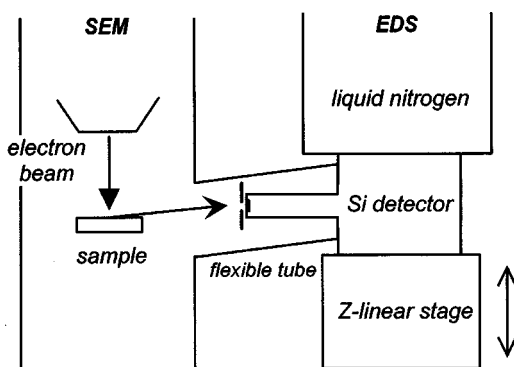


FIG. 2. Experimental setup of GE EPMA. The GE-EPMA equipment consists of SEM and EDS, which are connected with a flexible stainless-steel tube. Therefore, it is possible to move the EDS in the vacuum.

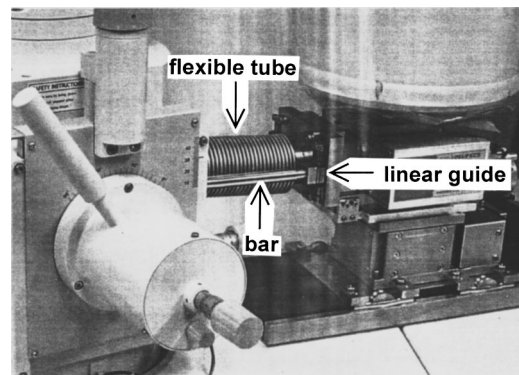


FIG. 3. Photograph of the flexible tube of the GE EPMA.

acteristic radiation intensity was automatically measured using this computer.

IV. SAMPLE

To demonstrate the analytical performance of the GE EPMA, particles of Pd–Se–Te were measured. Trace analysis of Se and Te in stainless-steel (or high-purity metals) samples is important because these elements influence the strength of the stainless steel. To analyze Se and Te, these elements have to be separated from the Fe matrix.¹⁴ As a result of the separation procedure using Pd, powders of Pd–Se–Te (2:1:1) are obtained.

Here, Pd–Se–Te particles were prepared as follows:^{14,15} Se and Te metal were dissolved in HNO_3 solution, and Pd metal was dissolved in $\text{HNO}_3\text{--HCl}$ (3:1) solution. The solutions of these elements (Pd:Se:Te=2:1:1) were transferred into an erlenmeyer flask. Then, 5 ml of H_2SO_4 were added, and the solution was heated to fume on a heating plate. After cooling at room temperature, the solution was diluted with 95 ml of water. Next, 2 g of ascorbic acid were added, and the solution was stood with a ground stopper at room temperature for 24 h. After standing, the Se–Te–Pd precipitate was collected through a membrane filter (pore size; $0.2 \mu\text{m}$). These Pd–Se–Te particles were suspended in ethanol solution, and then a small droplet of the suspension was deposited on a Au thin film using a pipette. The Au thin film (100 nm) was deposited on a Si wafer by the vacuum evaporation method. After drying, single particles were obtained on the Au–Si substrate.

V. RESULTS AND DISCUSSIONS

A single particle (diameter: about $2 \mu\text{m}$) of Pd–Se–Te was measured by GE EPMA. Figure 4 shows the gross intensities of Pd $L\alpha$, Te $L\alpha$, Au $L\alpha$, and Se $K\alpha$ lines as a function of exit angle. These curves were obtained with a step angle of 0.01° and a counting time of 400 s. Although it took totally about 12 h to measure this scan, the electron beam irradiated the same position of the particle during the measurement. Previously, we tried to measure this angular dependence for a Mg-salt particle.⁹ However, the exit angle was changed by manually tilting the sample holder at that time; therefore, the analyzed position was also changed, as a result, the real angle-dependent curve could not be obtained.

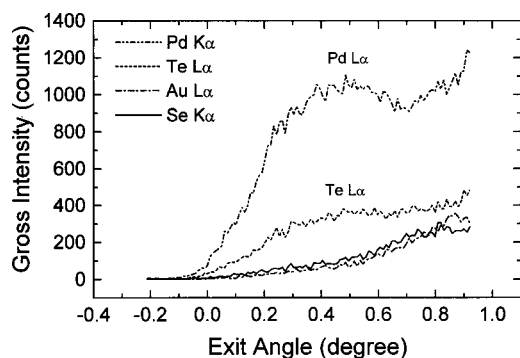


FIG. 4. Gross intensity of the characteristic x-ray intensity as a function of the exit angle. The sample was a single particle (about $2 \mu\text{m}$) of Pd–Se–Te deposited on a Au–Si substrate. These curves were measured at a step angle of 0.01° and for a counting time of 400 s at each angle.

The curves shown in Fig. 4 were obtained keeping the sample stable. Therefore, we can assume that the curves in Fig. 4 show the real angular dependence of the characteristic x-ray intensity.

As shown in Fig. 4, we obtained a clear difference between the angular-dependent curves for the particle (Pd $L\alpha$ and Te $L\alpha$) and for the substrate (Au $L\alpha$). In the case of x-ray emission from the particle, such x rays are emitted homogeneously to various directions. As shown in Fig. 4, Pd $L\alpha$ was detected below 0° due to the considerable height of the particle.⁹ At negative exit angles, characteristic x rays emitted from the single particle can be detected with low background from the substrate. On the other hand, it is theoretically expected that the x-ray intensities of Au L lines are very weak at grazing-exit angles, as described below.

The accelerating voltage was 20 keV, therefore, the electron beam could penetrate the small particle, and excite characteristic x rays from the Au–Si substrate. However, as shown in Fig. 4, the characteristic x rays of Au $L\alpha$ were very weak at the grazing-exit angles. We can explain these results by considering the critical angle. The critical angle (θ_c), where the characteristic x-ray intensity drastically increases, can be approximately described by the following equation: $\theta_c \doteq 1.65(\rho Z/A)^{1/2}/E$, where ρ is the density of the substrate, Z is the atomic number, A is the atomic weight, and E is the energy of the x rays.¹⁶ In the case of Au $L\alpha$, θ_c is about 0.47° . That is, Au $L\alpha$ x rays are expected to be weak at angles below 0.47° .

The x-ray spectra were taken for the same particle at different exit angles. Figure 5(a) presents an x-ray spectrum measured at an exit angle of 45° after the sample holder was tilted at 45° ; therefore, the incident angle of the electron beam was also 45° . In this spectrum, Si $K\alpha$ emitted from the Si wafer was dominant. Au $M\alpha$, Au $L\alpha$, and Au $L\beta$ were also detected; however, it was not possible to recognize Te $L\alpha$ and Se $K\alpha$ due to the large background intensity.

Figures 5(b) and 5(c) show x-ray spectra taken at the grazing-exit angles of 1.14° and 0.12° , respectively. Si $K\alpha$ was not detected in both spectra, in addition, any Au characteristic x-ray lines were not observed in the spectrum of Fig. 5(c). As previously pointed out,¹⁷ it is clearly shown that the characteristic x rays emitted from the substrate are drastically reduced at grazing-exit angles.

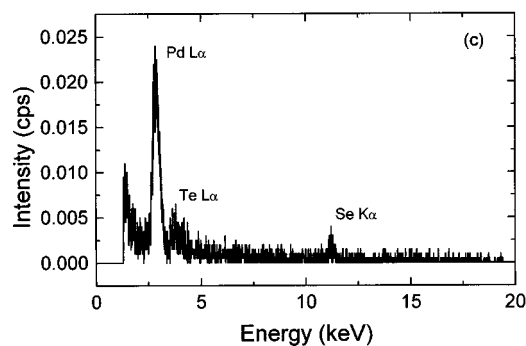
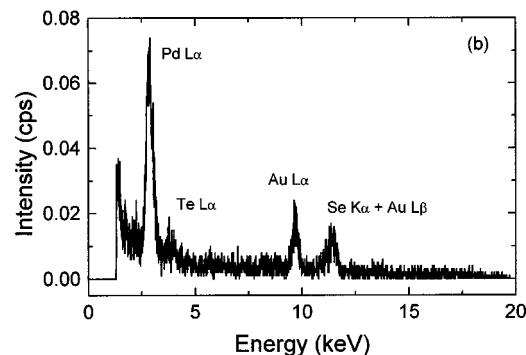
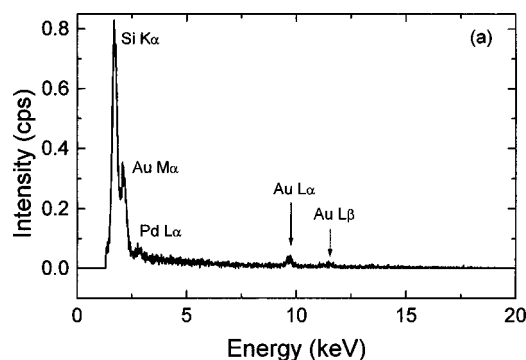


FIG. 5. X-ray spectra taken at different exit angles of (a) 45° , (b) 1.14° , and (c) 0.12° . The sample was the same Pd–Se–Te particle as that measured in Fig. 4. The counting times of (a), (b), and (c) were 500, 1000, and 2000 s, respectively.

Furthermore, in Fig. 5(b), it was difficult to distinguish Se $K\alpha$ (11.21 keV) from Au $L\beta$ (11.44 keV) due to the large Au $L\beta$ peak and the poor energy resolution of the EDS. Se $K\alpha$ was just overlapped on the shoulder of the Au $L\beta$ line. However, in Fig. 5(c), Au signals disappeared from the spectrum, as a result, the x rays of Pd $L\alpha$, Te $L\alpha$, and Se $K\alpha$ were detected with low background. Especially, Se $K\alpha$ could be first recognized after the Au characteristic x rays disappeared under the grazing-exit conditions. If the single particle deposited on the substrate includes the element that is also included in the substrate, it would be impossible to distinguish the x-ray radiations of such an element emitted from the particle and substrate by conventional EPMA. The grazing-exit measurement is useful in solving such an overlapping problem for particle analysis.

ACKNOWLEDGMENTS

One of the authors (Z.S.) was financially supported by the Japan Society for Promotion of Science (JSPS, No.

L00548). Part of this work was financially supported by JSPS Grant-in-Aid (C-11650827 and B-12554030) and by a grant from the Shimadzu Science Foundation. This work was performed under the research program (Nos. 234 and 313) at the Laboratory for Advanced Materials (LAM), Institute for Materials Research (IMR), Tohoku University.

- ¹V. D. Scott, G. Love, and S. J. B. Reed, *Quantitative Electron-Probe Microanalysis* (Ellis Horwood, New York, 1995), Chap. 13.
- ²G. F. Bastin, J. M. Dijkstra, and H. J. M. Heijligers, *X-Ray Spectrom.* **27**, 3 (1998).
- ³G. Love, *Microbeam Anal.* **3**, 239 (1994).
- ⁴J. L. Pouchou, *Mikrochim. Acta* **114/115**, 33 (1994).
- ⁵D. E. Newbury, *Microsc. Microanal.* **4**, 585 (1999).
- ⁶E. Boyes, *Adv. Mater.* **10**, 1277 (1998).
- ⁷E. Boyes, *Microsc. Microanal.* **6**, 307 (2000).
- ⁸I. Barkshire, P. Karduck, W. P. Rehbach, and S. Richter, *Mikrochim. Acta* **132**, 113 (2000).
- ⁹K. Tsuji, K. Wagatsuma, R. Nullens, and R. Van Grieken, *Anal. Chem.* **71**, 2497 (1999).
- ¹⁰K. Tsuji, Z. Spolnik, K. Wagatsuma, J. Zhang, and R. Van Grieken, *Spectrochim. Acta, Part B* **54**, 1243 (1999).
- ¹¹K. Tsuji, K. Wagatsuma, R. Nullens, and R. Van Grieken, *J. Anal. At. Spectrom.* **14**, 1711 (1999).
- ¹²S. Hasegawa, S. Ino, Y. Yamamoto, and H. Daimon, *Jpn. J. Appl. Phys., Part 2* **24**, L387 (1985).
- ¹³K. Tsuji, Z. Spolnik, K. Wagatsuma, R. Nullens, and R. Van Grieken, *Mikrochim. Acta* **132**, 357 (2000).
- ¹⁴T. Ashino, K. Takada, and K. Hirokawa, *Anal. Chim. Acta* **297**, 443 (1994).
- ¹⁵T. Ashino, K. Takada, and K. Hirokawa, *Anal. Chim. Acta* **312**, 157 (1995).
- ¹⁶R. Klockenkämper, *Total-Reflection X-Ray Fluorescence Analysis* (Wiley, New York, 1997), p. 30.
- ¹⁷K. Tsuji, Y. Murakami, K. Wagatsuma, and G. Love, *X-Ray Spectrom.* **30**, 123 (2001).